Eur Biophys J (2005) 34: 973–986
DOI 10.1007/s00249-005-0477-9

ARTICLE

Genrikh N. Berestovsky · Anatoly A. Kataev

Voltage-gated calcium and Ca^{2+}-activated chloride channels and Ca^{2+} transients: voltage-clamp studies of perfused and intact cells of *Chara*

Received: 7 September 2004 / Revised: 22 February 2005 / Accepted: 28 February 2005 / Published online: 22 June 2005

Abstract The voltage-clamp technique was used to study Ca^{2+} and Cl^- transient currents in the plasmalemma of tonoplast-free and intact *Chara corallina* cells. In tonoplast-free cells [perfused medium with ethylene glycol bis(2-aminoethyl ether)tetraacetic acid] long-term inward and outward currents through Ca channels consisted of two components: with and without time-dependent inactivation. The voltage dependence of the Ca channel activation ratio was found to be sigmoid-shaped, with about −140-mV activation threshold, reaching a plateau at $V > 50$ mV. As the voltage increased, the characteristic activation time decreased from approximately 10^3 ms in the threshold region to approximately 10 ms in the positive region. The positive pulse-activated channels can then be completely deactivated, which is recorded by the Ca^{2+} tail currents, at below-threshold negative voltages with millisecond-range time constants. This tail current is used for fast and brief Ca^{2+} injection into tonoplast-free and intact cells, to activate the chloride channels by Ca^{2+}. When cells are perfused with EDTA-containing medium in the presence of excess Mg^{2+}, this method of injection allows the free submembrane Ca^{2+} concentration, $[Ca^{2+}]_c$, to be raised rapidly to several tens of micromoles per liter. Then a chloride component is recorded in the inward tail current, with the amplitude proportional to $\left[Ca^{2+}\right]_c^2$. When Ca^{2+} is thus injected into an intact cell, it induces an inward current in the voltage-clamped plasmalemma, having activation–inactivation kinetics qualitatively resembling that in EDTA-perfused cells, but a considerably higher amplitude and duration (approximately 10 A m^{-2} and $\tau_{inact} \sim 0.5$ s at −200 mV). Analysis of our data and theoretical considerations indicate that the $[Ca^{2+}]_c$ rise during cell excitation is caused mainly by Ca^{2+} entry through plasmalemma Ca channels rather than by Ca^{2+} release from intracellular stores.

Keywords Ca channel · Cl channel · Calcium entry · *Chara* · Perfused cell

G. N. Berestovsky (✉) · A. A. Kataev
Institute of Cell Biophysics,
Russian Academy of Sciences, 142290
Pushchino, Moscow Region, Russia
E-mail: gberest@icb.psn.ru
Fax: +7-0967-330509

Introduction

The plasma membrane (plasmalemma) of Characean alga cells contains two types of ionic channels responsible for generating action potential: the voltage-gated Ca^{2+}-permeable and the Ca^{2+}-activated Cl channels (Lunevsky et al. 1977, 1983). Importantly, the Ca channels possess their own specific inactivation mechanism as in animal cells (Hille 2001). It is generally accepted that depolarization of the plasmalemma beyond a threshold voltage causes activation of Ca channels and accordingly an increase in the concentration of free cytoplasmic Ca^{2+}, $[Ca^{2+}]_c$. The rise of $[Ca^{2+}]_c$ leads to activation of Cl channels, giving rise to further depolarization of the plasmalemma and, in turn, to generation of action potential. Under physiological conditions in voltage-clamped plasmalemma, the activation–inactivation transient current includes both the calcium, i_{Ca}, and the chloride, i_{Cl}, components (Lunevsky et al. 1983; Kikuyama 2001). The amplitude of i_{Ca} is usually much smaller than that of i_{Cl}. Such interference of currents, as well as the dependence of i_{Cl} upon i_{Ca}, considerably hinder separate investigation of Ca and Cl channel properties in the intact cells, even if channel-specific inhibitors are used. This problem was to some extent bypassed by using perfused tonoplast-free cells (Williamson 1975; Tazawa et al. 1976; Tazawa et al. 1987). Such models allow separate recording of current through both calcium and chloride channels by varying the composition of the intracellular perfusion medium (PM). To record i_{Ca} under voltage-clamp conditions, calcium-free PM is typically used containing a sufficient concentration of Ca^{2+} chelator ethylene

glycol bis(2-aminoethyl ether)tetraacetic acid (EGTA), as well as Mg^{2+} and ATP to maintain the calcium channel activity (Shimmen and Tazawa 1977; Zherelova et al. 1985; Berestovskii et al. 1987; Shiina and Tazawa 1987a). Chloride channels were activated with PM containing a suitable concentration of free Ca^{2+} (Kataev et al. 1984, 1988; Shiina and Tazawa 1988; Mimura and Shimmen 1994). This cellular model allowed the investigation of many properties of both channel types, including *I–V* characteristics, selectivity, and pharmacology (Berestovskii et al. 1987; Tester 1990; Kikuyama 2001). Even though Ca channels were investigated within that cellular model in many studies, their kinetics properties were never assessed in detail. Besides, conditions were not established that would allow the activation of Cl channels by external Ca^{2+} entry through Ca channels, which is essential for making comparisons with those in the intact cell at similar voltage protocol on the plasmalemma. Such a comparison could be particularly useful for additional verification of the hypothesis maintained by a number of researchers (Thiel and Dityatev 1998; Biskup et al. 1999; Wacke et al. 2003) that membrane excitation is dominated by Ca^{2+} release from internal stores rather than by external Ca^{2+} entry.

This study primarily aims at developing an improved tonoplast-free cellular model, which should be more suitable to the intact cell, assessing this new model cell's properties, and a preliminary comparison with the properties of the intact cell. In this paper we report activation and deactivation kinetics of calcium channels in tonoplast-free *Chara corallina* cells, obtained under voltage-clamp conditions. We demonstrate an efficient method of fast and brief, pulse-driven Ca^{2+} injection into the cell through the previously activated plasmalemma calcium channels during their deactivation at negative voltage, so that injection is driven by the tail Ca^{2+} current. The method allows the activation of Ca^{2+}-dependent chloride channels in both tonoplast-free (in an EDTA-containing PM) and intact cells. Using this method, we show that i_{Cl} is proportional to the square of the cytoplasmic Ca^{2+} concentration, which supports our earlier data on *Nitellopsis* (Kataev et al. 1984; Berestovskii et al. 1987). We also present evidence that the Ca^{2+} concentration rise (above approximately 1 μM) in voltage-clamp experiments results mainly from the entry of external Ca^{2+}.

Materials and methods

Plant material

Internodal cells of *C. corallina* were used. Algae were cultured in a large tank containing a layer of pond mud. The tank was illuminated by a 40-W luminescent lamp (day/night rhythm of 14/10 h). One to 2 days prior to the experiment, internodal cells of 0.7–0.8 mm in diameter were isolated from neighboring cells and kept in artificial pond water containing 0.1 mM KCl, 1.0 mM NaCl, and 0.5 mM $CaCl_2$.

Intracellular perfusion

Intracellular perfusion was performed according to the method of Kataev et al. (1984). Tonoplast-free cells were prepared by replacing the cell sap with a medium containing the Ca^{2+}-chelating agents EGTA or EDTA (Williamson 1975; Tazawa et al. 1976). EGTA-containing PM was used to study the calcium current. The basic PM contained 5 mM EGTA, 6 mM $MgCl_2$, 10 mM CsCl, 1 mM ATP, 240 mM sucrose, 10 mM *N*-(2-hydroxyethyl)piperazine-*N*′-ethanesulfonic acid (HEPES)/NaOH, pH 7.3. The bathing medium was 0.1 mM KCl, 1 mM NaCl, 1.0 mM $CaCl_2$, 160–180 mM sucrose, and 1 mM HEPES/NaOH, pH 7.3.

To establish conditions for the $[Ca^{2+}]_s$ rise in the submembrane region, and therefore for Ca^{2+} activation of chloride channels by the inward calcium current, PM with EDTA in the presence of excess Mg^{2+} ($[Mg]_{tot} > [EDTA]_{tot}$) was used. The time constant of Ca^{2+} relaxation τ_r, in such a PM, if $[Ca]_{tot} \ll [Mg^{2+}]$, does not depend on $[Ca^{2+}]_{tot}$: $\tau_r = K_D^{Ca}\left([Mg]_{tot} - [EDTA]_{tot}\right) / [Mg]_{tot} K_D^{Mg} k_-^{Ca}$, where K_D^{Ca} and K_D^{Mg} are the dissociation constants for calcium and magnesium, respectively, and k_-^{Ca} is the dissociation rate constant for calcium. At neutral pH, $K_D^{Ca}/K_D^{Mg} \approx 10^{-2}$, k_-^{Ca} is about 1 s^{-1} at 25°C (Carr and Swartzfager 1975), so values of τ_r in the tens of milliseconds range may be achieved,

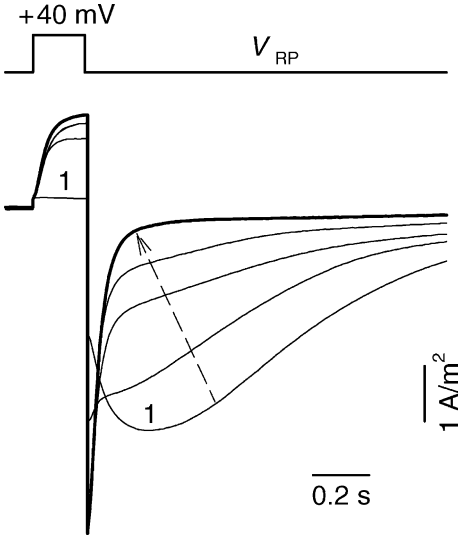

Fig. 1 Typical evolution of current during progressing destruction of the vacuolar membrane by a Ca^{2+} chelator [ethylene glycol bis(2-aminoethyl ether)tetraacetic acid]-containing perfusion solution. *Top* Protocol of voltage applied between the vacuole and the external medium. V_{RP} is the resting potential. *Curve 1* is for the cell with the intact tonoplast. The *arrow* indicates the final (after 10–15 min) shape of the current, for the cell with the completely destroyed tonoplast

depending on the $[EDTA]_{tot}/[Mg]_{tot}$ ratio and the temperature.

Tonoplast was removed according to the following procedure. The cell was placed into a three-compartment chamber (Andjus et al. 1994) and dried to decrease turgor. The central compartment was filled with the external medium. When the cell had almost lost its turgor, both its end were cut off, and the two side compartments were filled with PM, but to different levels to maintain the solution flow-through. Upon replacement of vacuolar sap by the perfusion solution, the flow-through was stopped for the entire duration of the experiment. Under such conditions, calcium channels of the plasmalemma retained their functional activity tens of minutes after tonoplast destruction. The latter process was monitored under voltage-clamp conditions by observing the change in the transient current in response to a short depolarizing pulse (Fig. 1). Upon tonoplast destruction, when the voltage remains applied to the plasmatic membrane only, the transient current exhibits a rise in its amplitude and a marked change in its time course, the latter becoming stationary (bold line in Fig. 1). This curve reflects the process of activation of Ca^{2+} channels upon plasmalemma depolarization, and the subsequent deactivation (see "Results").

Electrophysiology measurements

Voltage clamping of perfused cells was achieved by mounting the cells in a three-compartment chamber and passing a clamp current between external Ag/AgCl electrodes placed in one of the side compartments and the central compartment while monitoring the membrane voltage in the central compartment with two glass electrodes, placed near the cell wall in the central compartment and in the other side compartment (Kataev et al. 1984; Drinyaev et al. 2001). The clamped region of the cell in the compartment was 2-mm long.

Voltage clamping of intact cell plasmalemma was carried out according to the method of Lunevsky et al. (1983). A Dagan 8500 amplifier was used for voltage clamping. An IBM/AT 486 computer equipped with a PCL-718 AD/DA board and "Bio Quest" software was used. All experiments were carried out at room temperature (19–22°C).

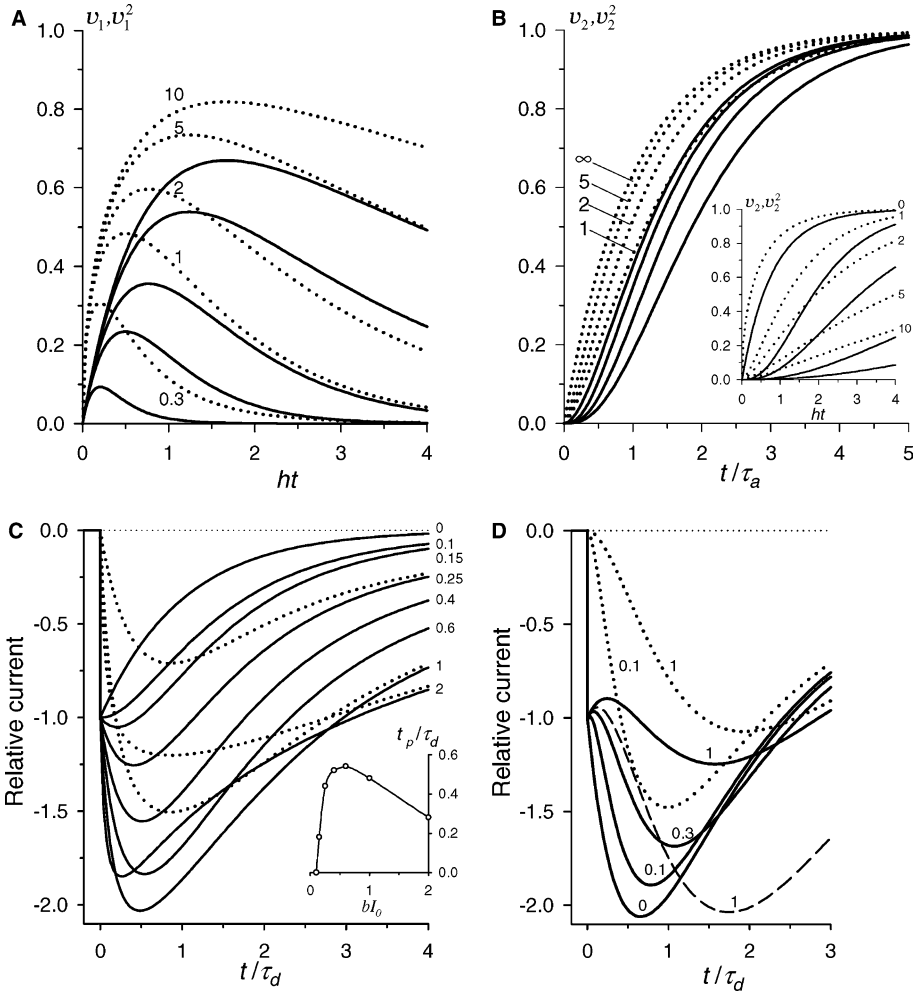

Fig. 2 Plots of the functions: **a** $v_1(t)$ (Eq. 5) and $v_1^2(t)$ (*solid lines*), **b** $v_2(t)$ (Eq. 6) and $v_2^2(t)$ (*solid lines*). The *numbers* beside the curves are the $h\tau_d$ (**a**) and $h\tau_a$ (**b**) values. **c** Theoretical curves of the relative tail current (*solid lines*) with the chloride (*dotted lines*) component $[i/I_0 = i_{Ca}/I_0 + I_{Cl}/I_0$, where $i_{Ca} = -I_0 \exp(-t/\tau_d)]$ calculated according to Eq. 9, for $a = 3$ and $h\tau_d = 0.1$. Values of bI_0 are shown next to the curves. *Inset* Dependence of the peak time of the current on bI_0. **d** Curves of i/I_0 and i_{Cl}/I_0 (*dotted lines*) drawn with allowance for the activation kinetics of chloride channels according to Eq. 10. $abI_0 = 1.4$ ($= 2.1$, *dashed line*), $\bar{v}_1^2(t)$ at $h\tau_d = 0.1$. Values of τ_{Cl}/τ_d are shown beside the curves

Theory

Time course of Ca^{2+} concentration in a tonoplast-free cell in response to Ca^{2+} influx

Consider Ca^{2+} diffusion into a semi-infinite medium from a planar source. Such an approach will not introduce a noticeable error into determining the Ca^{2+} concentration, $C(x,t)$, as a function of distance from the membrane, x, at any time, t, or the $C(x,t)$ as a function of time at various distances from the membrane, if the following conditions are satisfied (Thomas 1982, pp 50–51): (1) the distance from the membrane, x_0, does exceed about a quarter of the cell radius; (2) only the periods of time when most of the Ca^{2+} is within this distance will be considered. This is true for Dt/x_0^2 values up to at least 0.1, where D is the Ca^{2+} diffusion coefficient. With $D = 10^{-3}$ mm^2 s^{-1} and $x_0 = 0.1$ mm (i.e., cell radius of about 0.4 mm) this means that we can consider times up to 1 s.

Assuming, as the first approximation, that the rate of Ca^{2+} association to the buffer is proportional to the Ca^{2+} concentration, C, the diffusion equation will be obtained in the form (Crank 1975)

$$\frac{\partial C}{\partial t} = D\frac{\partial C}{\partial x^2} - hC, \tag{1}$$

where h is the association rate constant ($h = \tau_r^{-1}$ in the PM with EDTA, see "Materials and methods"). Its solution is sought for the following initial and boundary conditions: $C(x,0) = 0$, $D\partial C(0,t)/\partial x = -j(t)$, where $j(t)$ is the influx of Ca^{2+} ions ($j = i_{Ca}/2F$, F is Faraday's constant). Its general solution (Budak et al. 1956, p 313) is

$$C(x,t) = \frac{\exp(-ht)}{\sqrt{\pi D}}\int_0^t \frac{j(\tau)}{\sqrt{t-\tau}}\exp\left[h\tau - \frac{x^2}{4D(t-\tau)}\right]\mathrm{d}\tau.$$

For the case of interest, $x = 0$, the equation takes the form

$$C(x,t) = \frac{\exp(-ht)}{\sqrt{\pi D}}\int_0^t \frac{j(\tau)}{\sqrt{t-\tau}}\exp(h\tau)\mathrm{d}\tau. \tag{2}$$

Under voltage-clamp conditions, the Ca^{2+} influx, $j(t)$, can be generally represented as the sum of one constant component and several exponential components. For both component types, simple solutions are available for Eq. 2.

Consider two basic forms of the $j(t)$ function: (1) Ca^{2+} tail influx during deactivation of Ca channels

$$j_1 = J_0\exp(-t/\tau_d) \tag{3}$$

and (2) influx caused by activation of Ca channels

$$j_2 = J_0[1 - \exp(-t/\tau_a)], \tag{4}$$

where τ_d and τ_a are the deactivation time constant and the activation time constant, respectively. By solving Eq. 2 for both boundary conditions one obtains, in terms of dimensionless units,

$$v_1 \equiv C_1\sqrt{hD}\Big/J_0 = \frac{\sqrt{h\tau_d}\exp(-t/\tau_d)}{\sqrt{h\tau_d - 1}}\mathrm{erf}\sqrt{(h\tau_d - 1)t/\tau_d} \tag{5}$$

and

$$v_2 \equiv C_2\sqrt{hD}\Big/J_0 = \mathrm{erf}\sqrt{ht} - \frac{\sqrt{h\tau_a}\exp(-t/\tau_a)}{\sqrt{h\tau_a - 1}}\mathrm{erf}\sqrt{(h\tau_a - 1)t/\tau_a}, \tag{6}$$

where erf$z$ is the error integral of z. Its plot for $z = \sqrt{ht}$ is shown in the inset in Fig. 2b by the upper dotted line ($\tau_a = 0$). At $h\tau_d = 1$, $v_1 = 2\sqrt{ht}\exp(-ht)/\sqrt{\pi}$.

Plots of $v_1(t)$ and $v_2(t)$ functions and their squares are shown in Fig. 2a and b. The numbers beside the dotted lines denote the $h\tau_d$ and $h\tau_a$ values, respectively. From Fig. 2a one can see that, as τ_d increases at constant h, the peak values of $v_1(t)$ and, accordingly, $C_1(t)$, as well as the prepeak time, t_p, also increase, while the fall of the curves slows down. In contrast, the function $v_2(t)$ and, accordingly, $C_2(t)$, increase slower as τ_a is increased (Fig. 2b, inset). At $t \to \infty$, the function $v_2(t) \to 1$ at any value of τ_a. At $h\tau_a \to \infty$, $v_2(t) \to 1 - \exp(-t/\tau_a)$. Note that the increase of the function $v_2^2(t)$ (Fig. 2b, inset, *solid lines*) occurs with a certain lag, which grows as τ_a increases.

Time course of Ca^{2+}-activated Cl^- current

In the general case, when the submembrane (intracellular) Ca^{2+} concentration rise is sufficient for Cl channel activation, the transient current, i, will consist of two components: i_{Ca} and i_{Cl}.

The dependence of the chloride conductivity, g_{Cl}, on the intracellular Ca^{2+} concentration, is sigmoid-shaped with a Hill coefficient of about 2 (Kataev et al. 1984; Berestovskii et al. 1987), and accordingly is well fit by the Hill equation

$$g_{Cl} = g_{Clmax}\frac{C^2/K_D^2}{1 + C^2/K_D^2}, \tag{7}$$

where K_D is the apparent calcium dissociation constant. If $I_{Cl}(t)$ "instantly" follows the Ca^{2+} concentration, $C(t)$, then the expression $i_{Cl}(t) \sim g_{Cl}(t) \sim C^2(t)/[1 + C^2(t)/K_D^2]$ is valid, provided that the membrane voltage is constant. Taking into account Eq. 5in the case of $i_{Ca}(t) = -I_0\exp(-t/\tau_d)$, one obtains

$$C_1(t)/K_d = bl_0\bar{v}_1(t). \tag{8}$$

For the overall normalized current, one obtains

$$i(t)/I_0 = -\exp(-t/\tau_d) - \frac{abI_0\bar{v}_1^2(t)}{1 + b^2I_0^2\bar{v}_1^2(t)}, \tag{9}$$

where a is the proportionality constant, $b = v_{1\max}\left(2FK_D\sqrt{hD}\right)^{-1}$, and $\bar{v}_1 = v_1/v_{1\max}$. The second item of Eq. 9 reaches its maximal value at the same moment when $v_1(t) = v_{1\max}$ ($\bar{v}_1 = 1$) regardless of the values of other parameters including I_0.

At $bI_0 = 1$, as follows from Eq. 8, the Ca^{2+} concentration equals K_D at its maximum. In Fig. 2c, families of i/I_0 and i_{Cl}/I_0 curves are shown for several values of bI_0($a = 3$, $h\tau_d = 0.1$), demonstrating characteristic changes occurring in the current curves with growth of bI_0 caused by I_0 (b is constant). The changes are caused by the I_0 dependency of the relative current i_{Cl}/I_0 only, since i_{Ca}/I_0 (upper solid curve in Fig. 2c) does not depend on I_0. As I_0 increases when $bI_0 > \pi v_{1\max}^2/4a$, an extremum (peak) appears on the curves (in a range $0.1 < bI_0 < 0.15$ in Fig. 2c) and the prepeak time, t_p, initially increases as bI_0increases, but then falls (Fig. 2c, inset). With increasing I_0, the peak values of the relative currents first increase, and then decrease (compare curves with $bI_0 = 1$ and 2), and the fall of the current slows down. In the second case, when $i_{Ca} = -I_0[1 - \exp(-t/\tau_a)]$, the normalized chloride current, i_{Cl}/I_0, will be proportional to $cI_0v_2^2(t)/\left[1 + c^2I_0^2v_2^2(t)\right]$, where $c = \left(2FK_D\sqrt{hD}\right)^{-1}$ and its activation, as seen from the plot in Fig. 2b, will occur with some lag.

Calcium activation of g_{Cl}, as well as activation of other Ca^{2+}-dependent channels, is a multistage process (Hille 2001). To see how its kinetics affects the time course $i_{Cl}(t)$, we will use a single relaxation time constant τ_{Cl} as the first approximation. Then, the expression implicitly defining $g_{Cl}(t)$ will have a simple form $\tau_{Cl}dg_{Cl}/dt + g_{Cl} = f(t)$, where $f(t)$ is a function of $C(t)$. Then, if Ca^{2+} varies only negligibly so $C^2/K_D{}^2$is much smaller than unity (see Eq. 7), and if $i_{Ca}(t)$ is determined by Eq. 3, the equation defining $i_{Cl}(t)$ is obtained:

$$\tau_{Cl}\frac{di_{Cl}}{dt} + i_{Cl} = abI_0^2\bar{v}_1^2(t). \qquad (10)$$

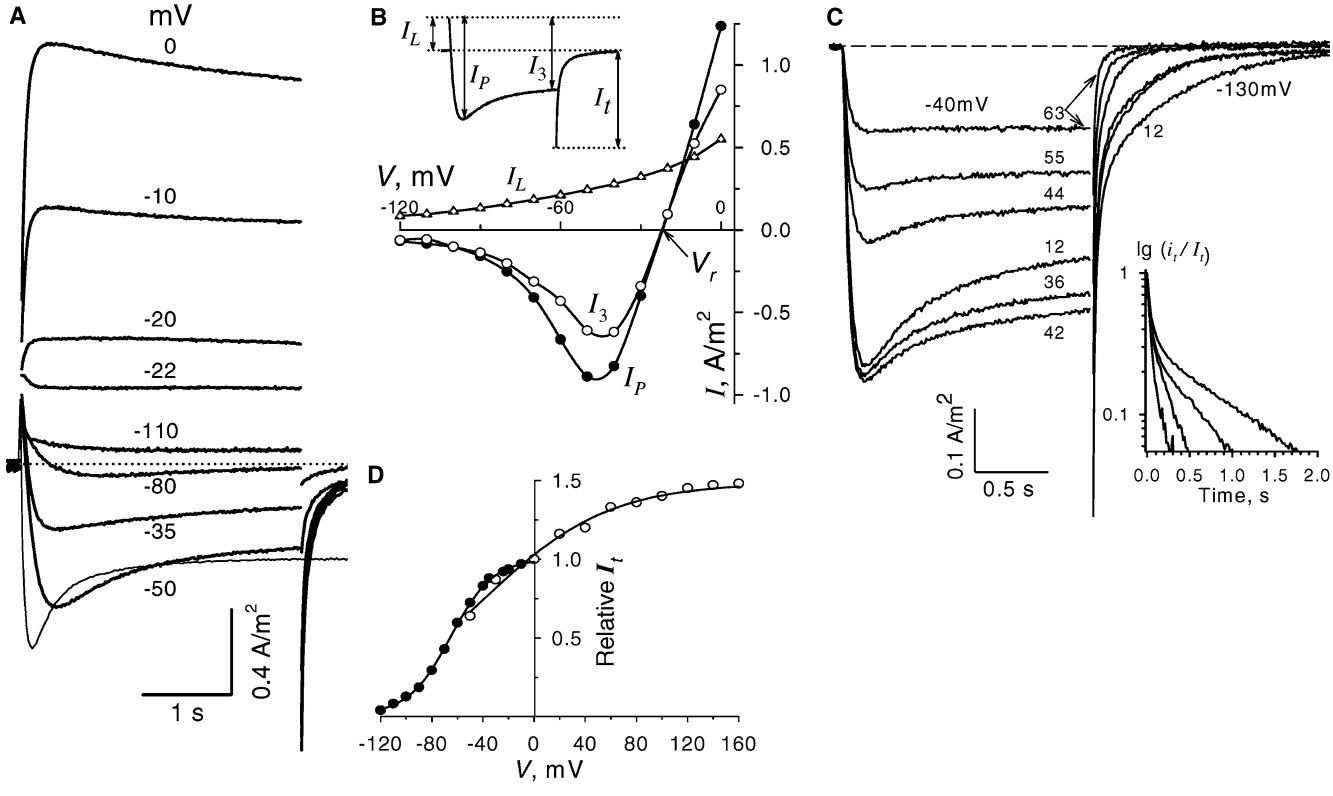

Fig. 3 **a** Membrane currents recorded with stepwise variation of voltage in a tonoplast-free cell of *Characorallina*. The *numbers* beside the curves indicate values of the clamped voltage. The holding voltage, V_h, is −130 mV. The *thin line* at the bottom is the track of the current for −50 mV voltage and the other cell with more pronounced peak of the inward current. **b** The *I–V* characteristics were drawn from the data of **a**. V_r is the reversion potential of the transient current. **c** Evolution of transient Ca currents before and after replacement of the intracellular medium (perfusion medium, *PM*, with EGTA) still containing the residual cytoplasm by pure PM, in the interval between pulses 42 and 44. The repetition period of the test pulses (−40 mV, 3.5 s) is 1 min. $V_h = -130$ mV. Leak currents were subtracted at −40 and −130 mV. For the other cell, $T = 17°C$. The *numbers* beside the curves denote successive numbers of the pulses. The series of pulses starts immediately after complete tonoplast destruction (see Fig. 1). *Inset* Relative tail currents of pulses 12, 42, 44, and 63. The $i_t(t)/I_t$ curves are adequately fit by a sum of two exponents with τ_1 about 40 ms and τ_2 decreasing from 1 (12) to 0.3 s (63). The relative amplitude of the slow component also decreases from 30 to 8%. **d** Activation curves (relative units) drawn from the tail current amplitudes, I_t, in the two cells. *Filled circles* the same cell as in **a**, *open circles* the other cell, voltage pulse length 370 μs

The results of solving Eq. 10 for the particular case allowing the general-case features to be revealed are shown in Fig. 2d. If $\tau_{Cl} \neq 0$, a typical delay visibly emerges in the activation of i_{Cl} and i, respectively. The lag in the current decreases with the increased fraction of i_{Cl} in the overall current (compare the solid and the dotted lines for $\tau_{Cl}/\tau_d = 1$). Besides, the peak values of both the chloride current and the overall current shift towards larger t values.

Results

Transient currents were recorded emerging in response to a depolarizing rectangular pulse applied to voltage-clamped tonoplast-free *Chara* cells, similar to the currents reported for *Nitellopsis* cells (Zherelova et al. 1985; Shiina and Tazawa 1987a; Beilby et al. 1993). In Fig. 3a a typical family of single-cell currents is shown as a function of voltage. The holding voltage V_h was −150 mV. The inward current was activated when the voltage exceeded the excitation threshold, $V\,z{\geq}-130$ to −140 mV, and the outward current was activated for $V \geq -20$ mV. Usually, the inward current slowly decayed (inactivating) to a certain level, but some cells exhibited a pronounced initial peak of the current (Fig. 3a, long trace at −50 mV). The initial current peak strongly decreased upon cell reperfusion, when the PM containing components of cytoplasm and the destroyed tonoplast was replaced by pure PM, as well as within 30–60 min after the start of the normal experiment (Fig. 3c). This suggests the existence of at least two types of Ca channels (high-voltage-activated and low-voltage activated, LVA, channels) differing in their regulation systems (MacRobbie and Banfield 1988; Thuleau et al. 1998), which is characteristic for Ca channels of most animal cells (Hille 2001; Catterall 2000; Dolphin 1998). An initial peak was noted for *Nitellopsis* cells as well (Shiina and Tazawa 1987a; Beilby et al. 1993). For voltages close to −20 mV, reversion of the transient current occurred. Its total disappearance at this voltage implies that a certain type of activating channel is responsible for the transient current, while another type of channel, whose activity remains unchanged during the pulse, is responsible for the remaining constant current (leakage current).

The transient current was proven to be the current passing through calcium channels (Zherelova et al. 1985; Berestovskii et al. 1987; Shiina and Tazawa 1987a), while the leakage current was caused mainly by potassium channels (Smith and Walker 1981; Sokolik and Yurin 1986; Tester 1990). The *I–V* relationship plotted from transient current amplitudes is shown in Fig. 3b. The curves for I_p and I_3 are similar in shape and both have minima at the same voltage, about −50 mV. The shape of the *I–V* relationship is conserved for longer (6–10 s) voltage pulses as well. It has the same *N*-shaped appearance as that of *Nitellopsis* (Zherelova et al. 1985; Shiina and Tazawa 1987a). Upon completion of the depolarizing pulse, deactivation of Ca channels occurred, as evidenced by the falling tail current (Fig. 3a, c). Importantly, as follows from Fig. 3c, the tail current's slow component decreases with time during depolarization simultaneously with the initial peak of the current. Such behavior of the current during depolarization, with channel activity retained after positive voltage pulses (not shown), indicates gradual loss of LVA-type Ca channel activity.

Activation of Ca channels

At constant voltage, the tail current amplitude, I_t, was proportional to the membrane conductivity, i.e., the activity of the Ca channels at the end of the depolarizing pulse (quantity of channels in an open state). A typical activation curve of Ca channels plotted from values of the tail currents is shown in Fig. 3d. The complete channel activation (curve plateau) appears to be reached for positive voltages of 150–200 mV. The steepest part of the activation curve lies in the −90- to −40-mV region. The fact that the two curves do not coincide in the region of their overlap is caused mainly by incomplete Ca channel activation at negative voltages within the 370-ms period. The characteristic time of Ca channel activation is voltage-dependent (Fig. 4). It decreases as the voltage is increased, as observed for most channels activated once the membrane has been depolarized (Hille 2001). Channel activation occurred with a certain lag (Fig. 4, inset). Such kinetics of the current is well approximated

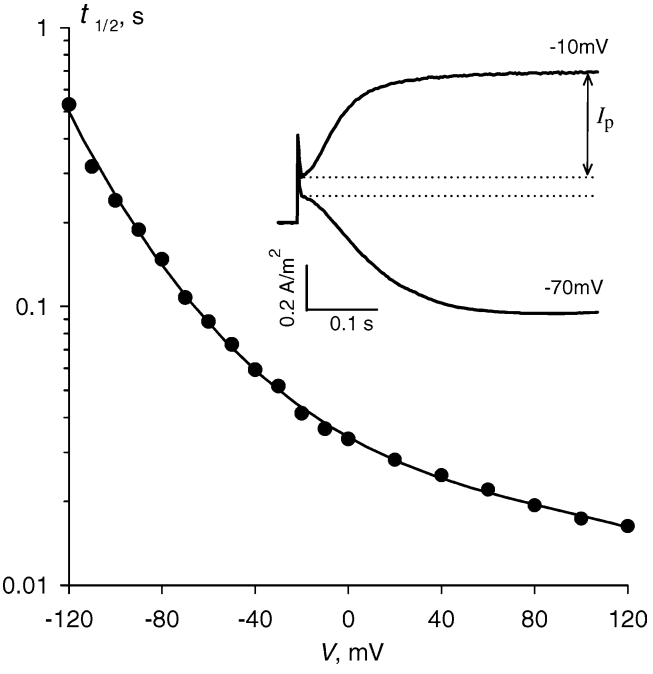

Fig. 4 Voltage dependence of the characteristic activation time of Ca channels. $t_{1/2}$ is the time when the current reaches $I_p/2$. $T = 24°C$. The *inset* shows the presence of the characteristic lag before activation of the inward and the outward currents

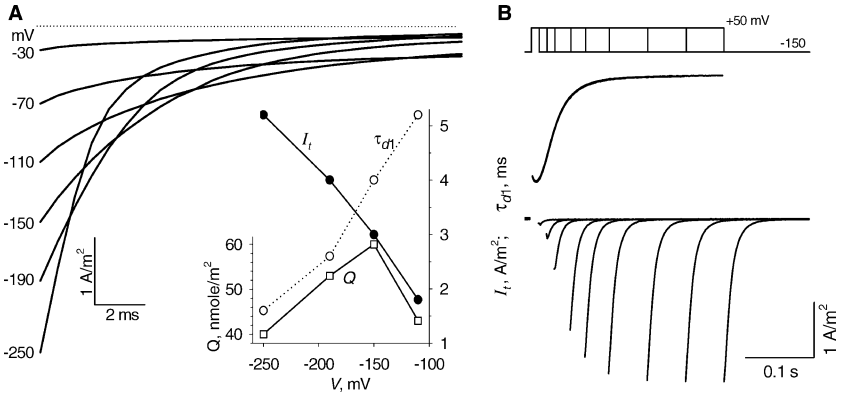

Fig. 5 **a** Tail currents for various voltages after a +50-mV, 100-ms test voltage pulse. Recordings start 0.6 ms after pulse completion. $T = 23°C$. *Inset* Voltage dependence of the tail current amplitude, I_t, the time constant of fast current component deactivation, τ_{d1} and the number of Ca^{2+} ions, Q, injected by this component of the current ($Q \sim I_t \tau_{d1}$). **b** Transient current for different lengths of the test pulse. *Top*, The voltage protocol. The 2-ms intervals following the voltage jumps are excluded from the current plots. **b** A technique for control of the tail current amplitude for the unchanged value of τ_d

by the known $m^p h$ expression (according to Hodgkin-Huxley), where $p = 1.3$–3 for the channels in question. For instance, the curves in the inset of Fig. 4 are approximated by the equation $i_{Ca} = A[1 - \exp(t/\tau_a)]^p$, with parameter values of $p = 2.8$ and 2.3, $\tau_a = 37$ and 79 ms for the −10- and −70-mV curves, respectively.

Deactivation of Ca^{2+} current

The deactivation kinetics of Ca channels from alga cell plasmalemma is voltage-dependent, as for animal cells. This dependency was detected from the tail currents obtained after preliminary activation of the Ca channels by a 50-mV, 0.2-s pulse (Fig. 5a). The transient component of the tail current is adequately approximated by two exponents (Fig. 3c, inset). The slower exponent has a considerably smaller amplitude, and becomes negligible if V is below the activation threshold of the Ca channels (below −150 mV).

For above-threshold V, the tail current also has, according to the I–V relationship (Fig. 3b), a constant component caused by incomplete deactivation of Ca channels. The voltage dependences of the tail current amplitude, I_t, and the time constant of the faster component of deactivation, τ_{d1}, are shown in the inset in Fig. 5a. The τ_{d1} values lie in the millisecond range and decrease with increasing hyperpolarization.

Thus, when Ca channels are completely deactivated ($V < -150$ mV), brief (pulse) injection of Ca^{2+} ions into cells occurs. Then, the quantity of the injected ions, Q, is determined by a simple expression: $Q = I_t \tau_d / 2F$. Note that the Q value decreases as the hyperpolarization increases for $V < -150$ mV (Fig. 5a, inset). In this Ca^{2+} ion injection protocol, the I_t value can be conveniently adjusted by varying the length of the positive prepulse within the time interval of Ca channel activation (Fig. 5b). Then, the τ_d value will remain unchanged, since deactivation will proceed at the same voltage. The proposed technique of dosed Ca^{2+} injection proved to be efficient in kinetics investigations of Ca^{2+}-dependent processes in both the perfused and the intact cells (see later).

After complete deactivation of the Ca channels of an EGTA-perfused cell, they Ca channels fully restore their initial properties, i.e., respond to the repeated depolarizing pulse with the same transient current as for the first pulse (Fig. 6). Thus, the refractory period in such a system is determined by the deactivation time of the channels only.

We shall now qualitatively estimate the maximal rise of Ca^{2+} concentration near the membrane, for both boundary conditions (Eqs. 3, 4). We assume $D = 10^{-3}$ mm^2 s^{-1}. For the tail current $I_t = 5$ A m^{-2} (at V = −200 mV), with $h = 30$ s^{-1} (EDTA-based PM), $\tau_d = 10$ ms, and $v_{1max} = 0.3$, Eq. 5 results in $C_1 \max = I_t v_{1max} / 2F\sqrt{hD} \approx 40$ μM. The plot (Fig. 2a) shows that when Ca^{2+} buffer with $h = 200$ s^{-1} ($h\tau_d = 2$) is used, $v_{1max} = 0.6$, so the concentration C_{1max} reduces to 30 μM. Thus, the tail calcium current can raise the free Ca^{2+} concentration near the membrane by several tens of micromoles, with the rise, importantly, requiring less than τ_d of time.

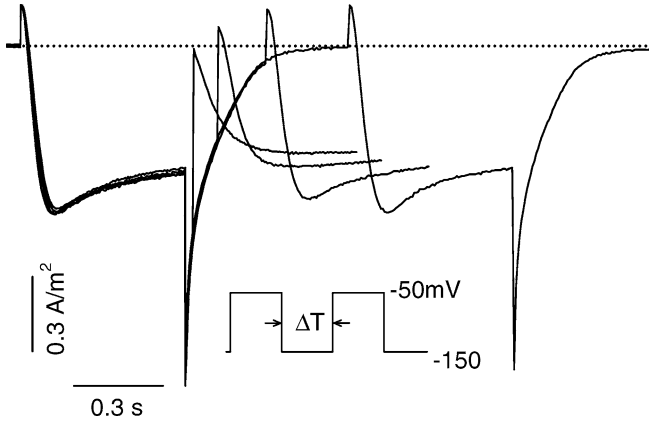

Fig. 6 Dependence of the degree of restoration of the Ca^{2+} current over the Δt interval between two identical voltage pulses

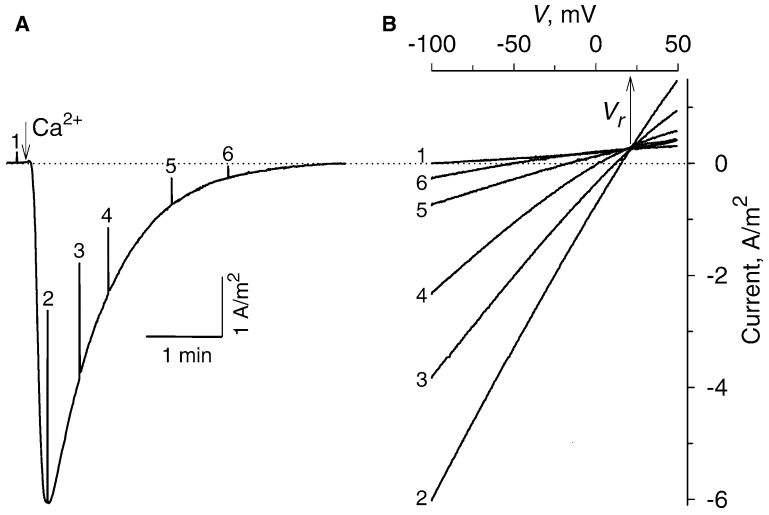

Fig. 7 Activation of plasmalemma's chloride conductance by intracellular Ca^{2+} after tonoplast removal. **a** Transient current for voltage clamped at −100 mV. *Numbered vertical lines*denote the moments at which sawtooth voltage pulses (150 mV, 30 ms) were applied to record instantaneous *I–V* plots, which are shown in **b**. **b***Curve 1* was obtained before perfusion solution with 35 μM Ca^{2+} was introduced. The intersection point of the curves indicates the reversion potential, V_r, for the current through the chloride channels. The scale of the current is the same for **a** and **b**. PM (mM): 2.0 EDTA, 1.62 $CaCl_2$, 1.5 $MgCl_2$, 12 KCl, 280 sucrose, 20 *N*-(2-hydroxyethyl)piperazine-*N*′-ethanesulfonic acid (*HEPES*)/KOH, pH 7.2. Bathing medium (mM): 1.0 $CaCl_2$, 1.0 NaCl, 0.1 KCl, 180 sucrose, 1.0 HEPES/NaOH, pH 7.4

When Ca^{2+} channels are activated via depolarization (Eq. 4), the Ca^{2+} concentration will be proportional to v_2, and will reach a plateau when $vv_2 = 1$ (Fig. 2b). Then, as follows from Eq. 6, $C_{2\max} = I_0/2F\sqrt{hD}$. Assuming $I_0 = 0.5$ A m^{-2}(at $V = -50$ mV), $\tau_a = 0.1$ s and $h = 30$ and 200 s^{-1}, we find that $C_{2max} \approx 15$ and 6 μM, respectively. These C_{2max} values take longer than $4\tau_a$ to reach (Fig. 2b), in this case more than 0.4 s. Comparing the first and the second cases of Ca^{2+} injection, we find that the maximal level reached by the Ca^{2+} concentration is several times higher, and is reached over an order of magnitude faster, in the first case than in the second case.

Ca^{2+}-activated Cl channels in tonoplast-free cells

Tonoplast-free Characean alga cells retain their Ca^{2+}-activated Cl channels (Kataev et al. 1984, 1988; Berestovskii et al. 1987; Shiina and Tazawa 1987b, 1988). A chloride (anionic), slowly inactivating (time constant about 1 min) current develops in those cells in response to replacement of the calcium-free perfusion solution by a Ca^{2+}-containing solution within them. In Fig. 7a, an example is presented of Cl channel activation by Ca^{2+} ions (35 μM) in *C. corallina* cells. The instantaneous *I–V* relationships (Fig. 7b), obtained at different moments of

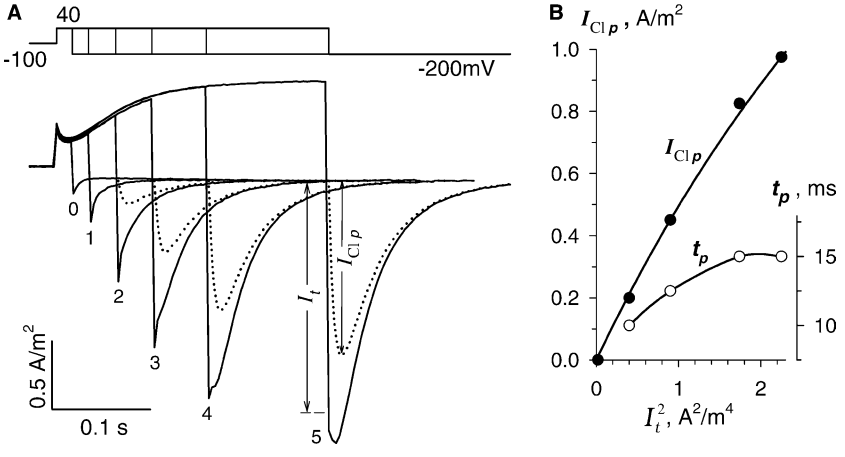

Fig. 8 **a** Tail currents and their chloride component (*dotted lines*) in a tonoplast-free cell versus the length of the activating +40-mV voltage pulse, as shown at the *top*. See text for details of the $i_{Cl}(t)$ calculation. $T = 8$°C. **b** Dependence of Cl^- current, I_{Clp}, and peak time, t_p, on the square of the calcium current amplitude, I_t. The *solid line* shows the fitting curve $AI_t^2/(1 + BI_t^2)$, where $A = 0.56$ A^{-1} m^2 and $B = 0.13$ A^{-2} m^4. PM (mM): 4 EDTA, 1 EGTA, 1 $CaCl_2$, 5 $MgCl_2$, 250 sucrose, 10 HEPES/NaOH, pH 7.3.

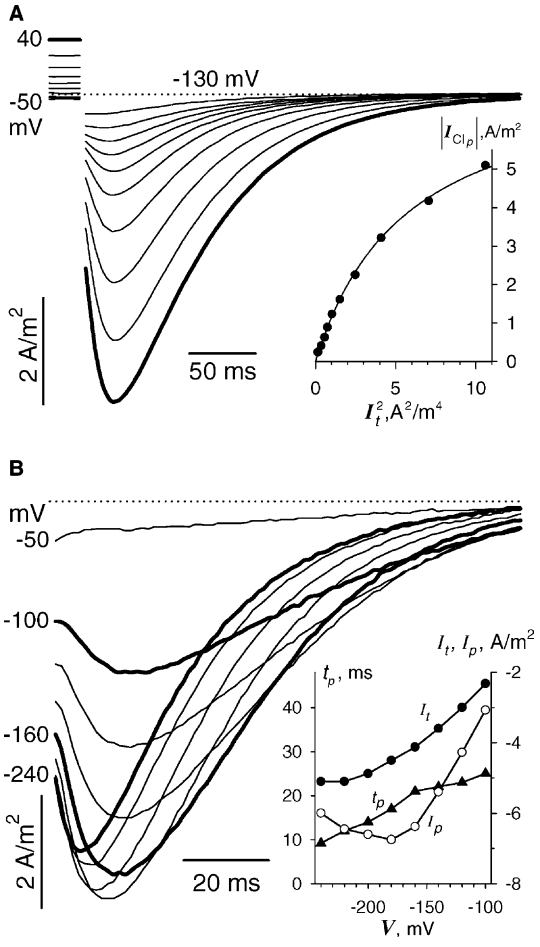

Fig. 9 Tail currents with the Cl^- component in tonoplast-free cells. **a** Tail currents after Ca channels have been activated by 0.5-s-long, −50- to +40-mV with 20-mV-increment voltage pulses. $V_h = -130$ mV. *Inset* I_{Clp} as a function of I_t^2(as in Fig. 8b). $A = 1.35$ A^{-1} m^2, $B = 0.184$ A^{-2} m^4. **b** Ca channels were opened at +50 mV for 0.2 s, and then stepped to different repolarizing voltages running from −240 to −100 mV. Traces at −100, −160, and −240 mV are in *bold*. The 4 ms following completion of the activating pulse was omitted in the tail current records. For the other cell, the *inset* shows the voltage dependences of the initial, I_t, and the peak, I_p, tail current values, as well as the time elapsed before the peak, t_p. PM (mM): 4 EDTA, 1 $CaCl_2$, 3.35 $MgCl_2$, 10 KCl, 240 sucrose, 20 HEPES/NaOH, pH 7.35. Bathing medium (mM): 1 $CaCl_2$, 1 NaCl, 0.1 KCl, 160 sucrose, 1 HEPES/NaOH, pH 7.3. T = 18°C

time, intersect at a single point corresponding to the transient current reversion. This implies that the selectivity of the ionic channels responsible for the transient current remains constant over time. The known Cl channel inhibitor, ethacrinic acid, suppresses that current, as observed for the *Nitellopsis* cells (Lunevsky et al. 1983; Kataev et al. 1984). The chloride current is also inhibited by avermectin B (Drinyaev et al. 2001). The threshold Ca^{2+} concentration at which the Cl channels in the perfused *Nitellopsis* cells are noticeably activated is on the order of 1 μM (Kataev et al. 1984; Shiina and Tazawa 1988).

The described procedure of Cl^-current activation by replacing the calcium-free perfusion solution by the Ca^{2+}-containing solution provides only a slow, second-range change of Ca^{2+} concentration in the cell. For faster, millisecond-range alteration of the submembrane Ca^{2+} concentration, we used the previously considered Ca^{2+} injection method using the tail current after preliminary activation of Ca channels by a positive voltage pulse. To ensure the $[Ca^{2+}]_c$ increase, the slowly Ca^{2+}-binding EDTA-based buffer was used. This buffer allows $[Ca^{2+}]_c$ to rise to tens of micromoles per liter as shown earlier. Transient currents for such Cl channel activation protocol are shown in Figs. 8a and 9. The biphasic shape of the tail current, i_t, suggests that, apart from the Ca^{2+} component, the chloride component is present ($i_t = i_{Ca} + i_{Cl} + i_L$, where i_L is the leakage current). When the Cl^- concentration in the PM is 10 mM higher than in the PM of Fig. 8, the contribution of the chloride component to the overall current becomes more pronounced (Fig. 9).

To determine the chloride contribution, i_{Cl}, to the overall tail current i_t and to establish the dependency of the chloride current peak value, I_{Clp}, on the amplitude of the calcium current, I_t, the following approach was used. The calcium tail current amplitude was altered by varying the length of the activating voltage pulse (similarly to Fig. 5b). The overall tail current was recorded at −200 mV, when i_{Ca} exponentially decayed to zero, and its contribution could be easily allowed for. Plots of the currents for such a protocol of their activation are shown in Fig. 8a. One can see that the shapes of the tail current curves change as the Ca channel activity grows. The tail current pulse marked 0 evidently reflects the capacitive current, i_c. Current 1 can, in the first approximation, be regarded as the exponentially decaying calcium current $i_{Ca}(t)$. Since, at V = const, the $i_{Ca}(t)$ kinetics does not depend on the current amplitude, the $i_{Cl}(t)$ curves can be calculated by subtracting the $i_c(t)$ and $i_{Ca}(t)$ currents, with proper correction for the changed amplitude of the latter, from tail currents 2–5 (Fig. 8a, dotted lines). In Fig. 8b, the dependence of the chloride current amplitude on the square of the amplitude of the calcium current is shown. It appears to be well approximated by a curve $AI_t^2/(1 + BI_t^2)$, where $B = 0.13$ A^{-2} m^4. Equation 8 and its analysis lead to $BI_t^2 = \left[Ca^{2+}\right]^2 / K_D^2$. Thus, when $BI_t^2 = 1$, the Ca^{2+} concentration will equal K_D, and the current, under the specified condition, will be $I_t^* = 1/\sqrt{B}$. As follows from the theoretical analysis (Fig. 2c), the quadratic dependence $I_{Clp}(I_t)$ also causes the small increase of t_p when I_t is increased (Fig. 8b).

Figure 9a shows that when the depolarizing pulse amplitude increases and thus the calcium conductivity of the membrane consequently increases (Fig. 3d) the peak value of the tail current, I_t, also rises. The time elapsed before the peak is reached, t_p, remained almost unchanged (cf. Figs. 9a, 2c), which agrees well with the independence of the deactivation time constant of the Ca^{2+} current, τ_d, on its amplitude, observed at

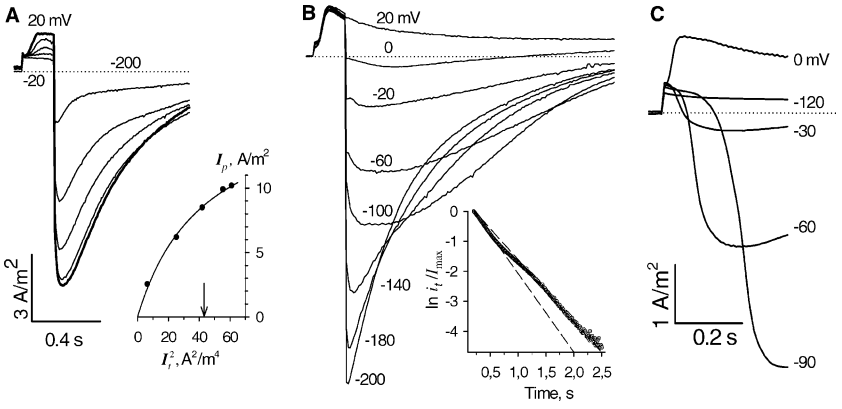

Fig. 10 Transient currents in the intact cell with clamped voltage at the plasmalemma. Bathing solution (mM): 1 $CaCl_2$, 1 tetramethylammonium chloride, 1 HEPES/NaOH, pH 7.3. $V_h = -200$ mV, 18°C. **a** Transients for various degrees of Ca^{2+} channel activation by −20 to +20-mV, 0.2-s-long pulses. The trace for +20 mV is in *bold*. *Inset* I_{p_1} as a function of I_t^2(as in Fig. 8b). $A = 0.4$ A^{-1} m^2, $B = 0.023$ A^{-2} m^4. The *arrow* denotes the value of $I_t^2 = 1/B \approx 43.5$ A^2 m^{-4}, at which the submembrane Ca^{2+} concentration is K_D (Eqs. 8, 9). **b** Tail currents after +20-mV, 0.2-s-long activating pulse, for various voltages. For the other cell, the *inset* shows a semilogarithmic plot of the tail current at −200 mV. The initial region of the curve reflects the exponential decay (0.4-s time constant) of the current. **c**Transients for various values of the voltage step. The voltage dependence of the time lag is demonstrated

V = const. A similar result was obtained if, at the constant pulse amplitude, a Ca channel inhibitor La^{3+} was used. To determine I_{Clp1} in this experiment, we utilized the data from the previous experiment (Fig. 8a), which show that the calcium component will drop approximately to $0.5I_t$ by the peak time of the overall current, t_p. Thus, the plot of I_{Clp} versus $I_t^2$was drawn assuming $I_{Clp} = I_p - 0.5I_t$. The fitting function in this case has the parameter values of $B = 0.184$ A^{-2} m^4 and, accordingly, $I_t^* \approx 2.3$ A m^{-2} . This value of I_t^* is equal, within the error margin, to that of the cell shown in Fig. 8, 2.8 A m^{-2} . As already mentioned, the Ca^{2+} concentration was found to increase to 30–50 μM when $I_t = 5$ A m^{-2}. Consequently, for $I_t^* = 2.5$ A m^{-2}, a rise of $[Ca^{2+}]_c = K_D$ to 15–25 μM should be expected. Such $K_D$values are close to those of the dissociation constant found for *Nitellopsis* (Kataev et al. 1984; Berestovskii et al. 1987).

In Fig. 9b, a family of tail current curves is shown which were obtained for different negative voltages and constant activating pulse amplitude (+50 mV). In this case, t_p decreases as the hyperpolarization is increased, I_p passes a maximum near −180 mV, and the initial current I_t (4 ms after the end of the pulse) grows monotonously (Fig. 9b, inset). Correlation is also manifested here with the behavior of the calcium tail current (Fig. 5a). At $V < -150$ mV, the τ_d value for that current decreases with increasing hyperpolarization, and $Q \sim I_t\tau_d$ also decreases, which leads to decreased I_p. The slower decrease of the tail current at $V > -150$ mV (Fig. 9b) reflects slower and incomplete Ca^{2+} current deactivation (Fig. 5a). In the curves for −100 to −160 mV, the tail current initially shows a steep rise, but then is clearly seen to develop within a certain lag caused by the time course of Ca^{2+} activation of Cl channels having a time constant of τ_{Cl} (see "Theory"). Comparison of the curves in Figs. 9b and 2d allows us to conclude that the τ_{Cl} value does not exceed several milliseconds.

The data presented show that values of both the amplitude and the time course of the current correlate sufficiently well with those of the calcium component of the current, in agreement with theoretical predictions (Fig. 2c). No noticeable deviations are observed in the current curves from those predicted by the theory. Therefore the $[Ca^{2+}]_c$ increase near the membrane is caused, albeit mainly, by Ca^{2+} influx from the external medium.

Currents in the intact cell

It is of interest to compare qualitatively the time course of the current in the intact cell (Fig. 10) with that of the tonoplast-free cell with the calcium and the chloride current components (Fig. 9). One can see that the two families of current curves are surprisingly similar in shape, considerably differing only in their amplitudes and time scales. In both cases, the peak values of the tail current at V = const increase, and the time intervals preceding the peaks, t_p, remain almost unchanged when the amplitudes of the Ca-channel-activating pulses are increased (cf. Figs. 9a, 10a). The constant t_p values were also observed in voltage-clamped cells when calcium channels were inhibited by La^{3+} (Biskup et al. 1999, Fig. 5). Besides, the curve shapes characteristically change, and times t_p decrease, when the plasmalemma hyperpolarization is increased (cf. Figs. 9b, 10b). All of this suggests that, for both the perfused cell and the intact cell, the tail current consists mainly of the calcium current and the Ca^{2+}-activated chloride current.

Consider also that the calcium current falls relatively rapidly in intact cells owing to an intrinsic mechanism of Ca channel inactivation (Lunevsky et al. 1983). Therefore, for all voltages, the tail current at the end of its decay

becomes equal to the leakage current. The process of Ca channel inactivation may be exemplified by the current curve at $V = +20$ mV with an inactivation time constant of about 0.35 s (Fig. 10b). The curve contains no chloride component of the current since, at this voltage, the calcium ions can hardly enter the cell through the Ca channels, as follows from the Goldman-Hodgkin–Katz equation, so there is nothing that could activate the Cl channels. The essential difference in the shapes of the current curve between $V > -140$ V and < -140 mV (Fig. 10b) is evidently related to two processes taking place in the former case, which are fast partial deactivation of Ca channels and their slower inactivation. In contrast, only the deactivation process takes place in the latter case. Note that similar changes in the shapes of the current curve occur in the tonoplast-free cell as well, in the same voltage ranges (Fig. 9b). Therefore, both the amplitude and the characteristic kinetics of the overall current are directly related to the corresponding characteristics of the Ca^{2+} current, which depend on the membrane voltage in a definite manner. This close correlation between currents provides evidence that the rise of the Ca^{2+} concentration in the cytoplasm, leading to i_{Cl}, activation, is mostly caused by Ca^{2+} influx from the outer medium, rather than release from intracellular stores. This conclusion agrees also with the $[Ca^{2+}]_o$ dependency of the overall current amplitude (Findlay 1964) and the increase of ^{45}Ca influx up to 25-fold when the membrane is depolarized by voltage clamping to values more positive then -100 mV (Reid et al. 1997), i.e., over the threshold of Ca channel activation.

As for the difference in current decay kinetics, it is evidently caused by the difference in the pathways of removing the injected Ca^{2+} from the membrane vicinity. In a tonoplast-free cell, Ca^{2+} is removed besides binding to buffer, mostly via Ca^{2+} diffusion into the cell volume. In contrast, in an intact cell where Ca^{2+} is accumulated in a thin (approximately 10-μm) layer of cytoplasm between the plasmatic and the vacuolar membranes, its concentration is reduced owing to three processes: (1) fast (less than 1-ms) binding to endogenous buffer (Naraghi et al. 1998), (2) diffusion towards the vacuolar membrane (dissipation of Ca^{2+} gradient), and (3) a slower process of Ca^{2+}-pumping and the Ca^{2+}/H^+ antiport, so the calcium is pumped both out of the cell and into the intracellular Ca^{2+} stores (Evans and Williams 1998; Sanders et al. 2002).

At room temperature and $V < -140$ mV, the current, which is predominantly the chloride current, drops (Fig. 10b), the time constant being within 0.4–0.6-s limits. A similar value (approximately 0.9 s) also characterizes the drop in the chemiluminescence intensity of the aequorin-injected *Chara* cell during the action potential (Kikuyama and Tazawa 1998, Fig. 2a). However, since the aequorin light emission intensity is, like the chloride conductance g_{Cl} of the membrane, proportional to the square of the Ca^{2+} concentration (Eckert and Tillotson 1979), the emission signal will reflect the g_{Cl} kinetics as well. The quadratic dependence of both parameters on $[Ca^{2+}]_c$ implies that the exponential decay of the Ca^{2+} concentration proceeds with a time constant about 2 times larger for the two previously described examples, i.e., 1–2 s. This also implies that, even if both i_{Cl} and the emission signal decrease many times, the Ca^{2+} concentration will still be comparatively high. For instance, when i_{Cl} (or the emission signal) is only 1% of the peak value, which is the noise level, $[Ca^{2+}]_c$ will still be as large as 10%.

From the $i_{Cl} \sim \left[Ca^{2+}\right]_c^2$ relationship, it also follows that, during stepwise depolarization of voltage-clamped cells, a lag phase should appear for Cl^- current activation (Fig. 2b, curves v_2^2). It is evident that this lag phase will actually be even longer owing to the lag phase in i_{Ca}activation (Fig. 4, inset). The overall lag phase will be longer for the larger time constant of Ca channel activation. The latter, in turn, will increase as the membrane voltage approaches the activation threshold of the Ca channel (Fig. 4). The family of curves in Fig. 10c, as well as the data of Kikuyama and Tazawa (1998) from experiments with aequorin-injected cells of *Characeae*, confirm those conclusions.

Discussion

A large number of Ca^{2+}-dependent processes take place in living cells. In investigating their kinetics with appropriate methods, rapid and controllable introduction of Ca^{2+} into the cell is crucial. One such method for cells possessing voltage-gated Ca channels is the method demonstrated herein of Ca^{2+} injection by the tail current through the Ca channels of a voltage-clamped cell previously activated by a positive voltage pulse. The method has a number of advantages:

1. During the activating positive pulse, only a small number of Ca^{2+} ions enter the cell since the voltage is close to its equilibrium value for Ca^{2+}; thus, Ca^{2+}-dependent processes in the cell will not have been started yet.
2. For voltages below the Ca channel activation threshold, the channels will be completely deactivated within a time considerably shorter than the time of their activation at above-threshold voltages. The deactivation process determining the tail current (Ca^{2+} injection kinetics) is exponential in nature, which allows us to estimate it easily and qualitatively, and to use it for analyzing diffusional processes in the cell.
3. This inward current is carried mainly by Ca^{2+} ions, even if univalent ions are present in as high as millimolar concentrations (Lunevsky et al. 1983; Hille 2001).
4. In the intact cell, the inherent channel inactivation mechanism is unable to affect the current during the brief channel deactivation time, which simplifies the analysis of Ca^{2+}-dependent processes.

5. The tail current amplitude is easy to change by varying the length of the activating pulse within the Ca channel activation time limits (Fig. 5b).
6. The initial jump of the tail current reflects the Ca channel activity, which allows us to monitor its changes under the action of external factors, including pharmacological preparations.
7. Injection of Ca^{2+} and Ca^{2+}-dependent processes, in particular chloride channel activation, proceed at constant membrane voltage, which simplifies their analysis.

On the whole, this method opens new opportunities for separate inhibitory analysis of Ca and Cl channels both in intact and in perfused Characean cells.

Our experiments show that the maximal peak currents in the intact cell (Fig. 10a, b) have values comparable to those of the peak chloride current observed when Cl channels are directly activated by 35 μM Ca^{2+} (Fig. 7b, curve 2). Consequently, the peak concentration of free Ca^{2+} near the membrane of the intact cell can reach tens of micromoles per liter, as in the EDTA–PM perfused cell (see earlier). On the other hand, most of the Ca^{2+} injected into the intact cell rapidly (less than 1 ms) binds to the endogenous buffer, B,, so the buffer is practically at chemical equilibrium with the local calcium concentration at every instant of time and at every point in the cytoplasm (Naraghi et al. 1998). Note that the fraction of free Ca^{2+}, i.e., the $[Ca^{2+}]/[CaB]$ ratio, is larger for larger $[Ca^{2+}]_{tot}$, and so is the apparent Ca^{2+} diffusion coefficient, D_{app} (Allbritton et al. 1992; Naraghi et al. 1998).

How does $[Ca^{2+}]$ near the plasmalemma reach the concentration of tens of micromoles per liter in the intact cell where the endogenous buffer is on the order of 100 μM? In our case, the tail current with $I_t \sim 10$ A $m^{-2}$is injecting the quantity of ions $Q = I_t \tau_d / 2F \approx 5 \times 10^{-4}$ mol μm l^{-1} in $\tau_d \sim 10$ ms. The corresponding equilibrium overall Ca^{2+} concentration, Q/l, will be 50 μM ($l = 10$ μm). The spatial distribution of the Ca^{2+} concentration, $C(x,t)$, is described, as a first approximation, by the equation $C(x,t)/C(0,t) = \exp\left(-x^2/4D_{app}t\right)$ (Allbritton et al. 1992). Accordingly, the range of action of a spatially localized impulse of Ca^{2+}can be approximated by the equation $s \approx 2\left(D_{app}\tau_d\right)^{1/2}$. Assuming the maximal value $D_{app} = 200$ μm^2 s^{-1}(Allbritton et al. 1992), we find $s \approx 3$ μm, whence $\Delta\left[Ca^{2+}\right]_{tot} = Q/s \approx 170\ \mu$M. Thus, the high Ca^{2+}concentration in a thin layer adherent to the membrane results from its binding by the buffer. For 200 (300) μM buffer concentration and the 10 μM Ca^{2+} dissociation constant, we obtain $[Ca^{2+}] = 25$ (10) μM, respectively. The minimal characteristic dissipation time, τ_{dis}, of the $[Ca^{2+}]$ gradient can be found using an analogous approximation, $\tau_{dis} = l^2/4D_{app} \sim$ 0.1 s. For comparison, according to Allbritton et al. (1992), cytosolic extract from oocytes exhibits a free Ca^{2+} concentration of approximately 20 μM at $[Ca^{2+}]_{tot} = 100$ μM. As for the dissipation time, even in 12-μm-diameter adrenal chromaffin cells, the Ca^{2+} gradient diffusionally dissipates over several hundred milliseconds to leave a uniformly elevated Ca^{2+} concentration, which decays to rest over several seconds (Marengo and Monck 2000).

The number of Ca^{2+} ions, Q, entering the cell through Ca channels during the action potential is of special interest. We will now evaluate the value of Q for the external Ca^{2+} concentration of 1 mM. In such a solution, the peak value of the action potential is −40 mV (Fig. 7a of Findlay and Hope 1964), and this voltage level persists within the initial 0.5 s. During the same period of time, $[Ca^{2+}]_c$ reaches its maximal value (Kikuyama and Tazawa 1998). Therefore, the Q value at $V = -40$ mV must be determined. As seen from Fig. 10b, when Ca channels are briefly (0.2 s) activated by a +20-mV pulse, the initial value of the tail current, I_t, will be about 15 A m^{-2} at −200 mV voltage. When the channels are activated by the voltage of interest, −40 mV, the current I_t will be about two thirds of the value at +20 mV according to the activation curve (Fig. 3d), i.e., about 10 A m^{-2} . Since the Goldman-Hodgkin–Katz equation establishes the almost linear voltage dependence of the Ca^{2+} current through the calcium channel at $V < -40$ mV, we obtain, for −40 mV, $I_t(-40) = I_t(-200)40/200$ A $m^{-2} = 3$ A m^{-2}. The calcium channels in the intact cell have an inactivation mechanism causing an exponential decrease of $i_{Ca}(t)$ with an inactivation time constant of $\tau_{in} \sim 10^{-1}$ s (Lunevsky et al. 1983). For a rough estimate, we assume $i_{Ca} = I_t \exp(-t/\tau_{in})$. Now, assuming also $I_t \sim 1$ A $m^{-2}$and $\tau_{in} \sim 10^{-1}$ s and following the logic of the previous calculation, we obtain uniformly $[Ca^{2+}]_{tot} = Q/l \sim 50$ μM. Thus, the contribution of i_{Ca} to the peak of the free Ca^{2+} concentration during the action potential will be no less than several micromoles per liter (at $[Ca^{2+}]_i \sim 1$ mM), i.e., much larger than the threshold of Cl channel activation by Ca, which is approximately 1 μM (Kataev et al. 1984; Shiina and Tazawa 1988). This conclusion is also confirmed by the estimate of the Ca^{2+} concentration rise during the action potential in *Chara* (6.7 μM) and *Nitella* (43 μM) cells (Williamson and Ashley 1982), as well as in *Nitellopsis* cells (approximately 20 μM) (Lunevsky et al. 1983).

The estimate of the concentration rise near the membrane for different regimes of Ca^{2+} injection neglected the cytoplasm heterogeneity. In reality, the Ca^{2+}concentration will be higher since a considerable part of the cytoplasm volume, particularly the ectoplasm volume, is occupied by organelles like chloroplasts and endoplasmic reticulum. Accordingly, the volume available for free diffusion of Ca^{2+} ions will be smaller than the total cytoplasm volume, and their concentration in the cytosol will be higher than the value calculated with respect to the total volume.

In our discussion of the Ca^{2+}transient in the cell resulting from Ca^{2+} influx through plasma membrane Ca channels, we concluded that the total currents recorded are quite closely correlated with Ca^{2+}current parameters. Therefore, the rise of the cytoplasmic Ca^{2+}

concentration near the membrane is mainly caused by its entry from the outside medium. The same conclusion was made by Tazawa and Kikuyama (2003) following detailed analysis of their inhibitor assays as well as data of other researchers.

These considerations, however, do not rule out the possible contribution of Ca^{2+} release from intracellular stores, particularly resulting from activation of Ca^{2+}-release channels of inositol 1,4,5-triphosphate (IP_3) receptors, as assumed by several workers (Thiel and Dityatev 1998; Plieth et al. 1998; Biskup et al. 1999; Wacke et al. 2003). However, this contribution is possible only within a narrow Ca^{2+} concentration range. In the presence of IP_3, the opening of IP_3 receptor channels is *stimulated* by small Ca^{2+} rises above rest but is *inhibited* when $[Ca^{2+}]_c$ reaches the micromolar range (Hille 2001). This is confirmed by the fact that the Ca^{2+} concentration rise owing to its release from intracellular stores, for various methods of release stimulation, does not usually exceed approximately 1 μM for both animal cells (Avdonin and Tkachuk 1994; Broad et al. 1999; Muallem et al. 1989) and plant cells (Miller and Sanders 1987; Knight 2000; Staxen et al. 1999). Therefore, those channels can be activated only at the very start of the stimulus, i.e., until free $[Ca^{2+}]$ reaches the micromolar level, or at the end of $[Ca^{2+}]_c$ decay, when it drops down to that level. Particularly, this may happen during the refractory period, or if the Ca^{2+} influx is small, as happens when $[Ca^{2+}]_o$ is small or near the activation threshold of Ca channels.

Can $[Ca^{2+}]_c$ rise to 1 μM owing to its release from a store depolarize the plasma membrane via activating the Cl channels up to the −120- to −140-mV activation threshold of its Ca channels? Assuming the quadratic dependence of g_{Cl} on $[Ca^{2+}]_c$ (Eq. 8) remains valid even for a Ca^{2+} concentration much lower than K_D, we obtain $g_{Cl} = g_{Clmax}\left[Ca^{2+}\right]_c^2 \Big/ K_D^2$. For *Nitellopsis*, $K_D \approx$ 20 μM, $g_{Clp} = i_{Clp}/(V - E_{Cl}) = 6\ \text{A m}^{-2}/150\ \text{mV} =$ 40 S m^{-2} (Kataev et al. 1984). Thus, at $[Ca^{2+}]_c = 1$ μM, the conductivity $g_{Cl} = 0.1$ S m^{-2}. Onset of chloride conductivity should lead to plasmalemma depolarization by $\Delta V = (E_{Cl} - V_{RP})/(1 + g_m/g_{Cl})$, where g_m is the conductivity of the resting plasmalemma, which usually is about 1 S m^{-2}. E_{Cl} and the resting potential, V_{RP}, are 40 and −160 mV, respectively. By substituting all the equation parameters, we find that a $[Ca^{2+}]_c$ increase to 1 μM due to intracellular sources will lead to membrane depolarization by approximately 20 mV. From this example, it follows that a receptor potential, ΔV, on the membrane within several tens of millivolts can be induced by various stimuli leading to Ca^{2+} release from stores. However, if the depolarization is sufficient for activating the plasmalemma Ca channels, then further development of the action potential is dominated instead by Ca^{2+} influx, according to the commonly accepted mechanism (Kikuyama 2001). It is this sequence of events that is likely to occur during generation of the action potential caused by the sufficiently massive Ca^{2+} release from intracellular stores under the action of various stimuli, e.g., mechanical (Haley et al. 1995; Knight et al. 1992; Shimmen 1997; Kikuyama and Tazawa 2001; Shepherd et al. 2002) or osmotic (Tazawa et al. 1994; Kikuyama 2001).

One other possible source of Ca^{2+} is the vacuole. If the cytoplasm's potential is positive with respect to the vacuole ($V_{cv} > 0$), the so-called slow-activating vacuolar (SV) channels are activated, which are Ca^{2+}-permeable (Lunevsky et al. 1983; Bewell et al. 1999). Accordingly, Ca^{2+} influx from the vacuole is possible through the SV channels. This is a probable cause of the occasionally observed lagged additional activation of inward chloride current when the plasma membrane is voltage-clamped (our observations herein; Beilby et al. 1993), since the inward current-caused $\Delta V_{cv} > 0$ adds to the background V_{cv}, which falls over time ($V_{cv} \rightarrow E_{Cl} \sim -40$ mV) (Findlay and Hope 1964) because of Ca^{2+} activation of the chloride channels of the vacuolar membrane (Lunevsky et al. 1983). Thus, while the intracellular calcium clearly contributes excitation to Characean cells, the nature and the extent of this contribution require further study.

Acknowledgements We are grateful to Victor Sivozhelezov for useful discussion and help during preparation of the manuscript. This work was partly supported by a grant from the Russian Foundation of Basic Research (grant no. 99 04 48553).

References

Allbritton NL, Meyer T, Stryer L (1992) Range of messenger action of calcium ion and inositol 1,4,5-triphosphate. Science 258:1812–1815

Andjus PR, Kataev AA, Alexandrov AA, Vučelič D, Berestovsky GN (1994) D_2O-induced ion channel activation in *Characeae* at low ionic strength. J Membr Biol 142:43–53

Avdonin PV, Tkachuk VA (1994) Receptors and intracellular calcium. Nauka, Moscow (in Russian)

Beilby MJ, Mimura T, Shimmen T (1993) The proton pump, high pH channels, and excitation: voltage clamp studies of intact and perfused cells *Nitellopsis obtusa*. Protoplasma 175:144–152

Berestovskii GN, Zherelova OM, Kataev AA (1987) Ionic channels in Characean algal cells. Biophysics 32:1101–1120

Bewell MA, Maathuis FJM, Allen GJ, Sanders D (1999) Calcium-induced calcium release mediated by a voltage-activated cation channel in vacuolar vesicle from red beet. FEBS Lett 458:41–44

Biskup B, Gradmann D, Thiel G (1999) Calcium release from $InsP_3$-sensitive stores initiates action potential in *Chara*. FEBS Lett 453:72–76

Broad LM, Armstrong DL, Putney JW (1999) Role of the inositol 1,4,5-triphosphate receptor in Ca^{2+} feedback inhibition of calcium release-activated calcium current (I_{crac}). J Biol Chem 274:32881–32888

Budak BM, Samarsky AA, Tikhonov AN (1956) Book of mathematical physics problems. Nauka, Moscow (in Russian)

Carr JD, Swartzfager DG (1975) Kinetics of the ligand exchange and dissociation reactions of calcium–aminocarboxylate complexes. J Am Chem Soc 97:315–321

Catterall W (2000) Structure and regulation of voltage-gated Ca^{2+} channels. Annu Rev Cell Dev Biol 16:521–555

Crank J (1975) The mathematics of diffusion. Clarendon, Oxford, p 329

Dolphin AC (1998) Mechanisms of modulation of voltage-dependent calcium channels by G proteins. J Physiol 506:3–11

Drinyaev VA, Mosin VA, Kruglyak EB, Sterlina TS, Victorov AV, Kataev AA, Berestovsky GN, Kokoz YuM (2001) Effect of

avermectins on Ca^{2+} -dependent chloride current of plasmalemma of *Chara corallina* cells. J Membr Biol 182:71–79
Eckert R, Tillotson D (1979) Calcium entry and the calcium-activated potassium systems of molluscan neurones:voltage clamp studies on aequorin-injected cells. In: Ashley CC, Campbell AK (eds) Detection and measurement of free Ca^{2+} in cells. Elsevier, Amsterdam New York Oxford, pp 203–217
Evans DE, Williams L (1998) P-type calcium ATPases in higher plants—biochemical, molecular and functional properties. Biochim Biophys Acta 1376:1–25
Findlay GP (1964) Ionic relations of cells of *Chara australis*. VIII. Membrane currents during a voltage clamp. Aust J Biol Sci 17:388–399
Findlay GP, Hope AB (1964) Ionic relations of cells of *Chara australis*. VII. The separate electrical characteristics of the plasmalemma and tonoplast. Aust J Biol Sci 17:62–77
Haley A, Russell AJ, Wood N, Allan AC, Knight M, Campbell AK, Trewavas AJ (1995) Effects of mechanical signaling on plant cell cytosolic calcium. Proc Natl Acad Sci USA 92:4124–4128
Hille B (2001) Ionic channels of excitable membranes. Sinauer, Sunderland MA
Kataev AA, Zherelova OM, Berestovsky GN (1984) Ca^{2+} -induced activation and irreversible inactivation of chloride channels in the perfused plasmalemma of *Nitellopsis obtusa*. Gen Physiol Biophys 3:447–462
Kataev AA, Zherelova OM, Berestovskii GN (1988) Effect of charged local anaesthetics on inactivation of Ca^{2+} -activated Cl^--channels of Characean algae. Biophysics 33:1076–1084
Kikuyama M (2001) Role of Ca^{2+} in membrane excitation and cell motility in Characean cells as a model system. Int Rev Cytol 201:85–114
Kikuyama M, Tazawa M (1998) Temporal relationship between action potential and Ca^{2+}transient in Characean cells. Plant Cell Physiol 39:1359–1366
Kikuyama M, Tazawa M (2001) Mechanosensitive Ca^{2+} release from intracellular stores in *Nitellaflexilis*. Plant Cell Physiol 42:358–365
Knight H (2000) Calcium signaling during abiotic stress in plants. Int Rev Cytol 195:269–324
Knight MR, Smith SM, Trewavas AJ (1992) Wind-induced plant motion immediately increases cytosolic calcium. Proc Natl Acad Sci USA 89:4967–4971
Lunevsky V, Aleksandrov A, Berestovsky G, Volkova S, Vostrikov I, Zherelova O (1977) Ionic mechanism of excitation of plasmalemma and tonoplast of characean algal cells. In: Thellier M et al (eds) Transmembrane ionic exchanges in planta. University de Rouen, Paris, pp 167–172
Lunevsky VZ, Zherelova OM, Vostrikov IY, Berestovsky GN (1983) Excitation of *Characeae* cell membranes as a result of activation of calcium and chloride channels. J Membr Biol 72:43–58
MacRobbie EAC, Banfield J (1988) Calcium influx at the plasmalemma of *Chara corallina*. Planta 176:98–108
Marengo FD, Monck JR (2000) Development and dissipation of Ca^{2+} gradients in adrenal chromaffin cells. Biophys J 79:1800–1820
Miller AJ, Sanders D (1987) Depletion of cytosolic free calcium induced by photosynthesis. Nature 326:397–400
Mimura T, Shimmen T (1994) Characterization of the Ca^{2+} -dependent Cl^--efflux in perfused *Chara* cells. Plant Cell Physiol 35:793–800
Muallem S, Pandol SJ, Beeker TG (1989) Hormone-evoked calcium release from intracellular stores is a quantal process. J Biol Chem 264:205–212
Naraghi M, Müller TH, Neher E (1998) Two-dimensional of the cellular Ca^{2+} binding in bovine chromaffin cells. Biophys J 75:1635–1647
Plieth C, Sattelmacher B, Hansen U-P, Thiel G (1998) The action potential in *Chara*-Ca^{2+} release from internal stores visualized by Mn^{2+} -induced quenching of fura-dextran. Plant J 13:167–175
Reid RJ, Tester MA, Smith FA (1997) Voltage control of calcium influx in intact cells. Aust J Plant Physiol 24:805–810
Sanders D, Pelloux J, Brownlee C, Harper J (2002) Calcium at the crossroads of signaling. Plant Cell Suppl 14:S401–S417
Shepherd VA, Beilby MJ, Shimmen T (2002) Mechanosensory ion channels in charophyte cells: the response to touch and salinity stress. Eur Biophys J 31:341–355
Shiina T, Tazawa M (1987a) Demonstration and characterization of Ca^{2+} channel in tonoplast-free cells of *Nitellopsis obtusa*. J Membr Biol 96:263–276
Shiina T, Tazawa M (1987b) Ca^{2+} -activated Cl^--channel in the plasmalemma of *Nitellopsis obtusa*. J Membr Biol 99:137–146
Shiina T, Tazawa M (1988) Ca^{2+} -dependent Cl^--efflux in tonoplast-free cells of *Nitellopsis obtusa*. J Membr Biol 106:135–139
Shimmen T (1997) Studies on mechanoperception in Characean cells: pharmacological analysis. Plant Cell Physiol 38:139–148
Shimmen T, Tazawa M (1977) Control of membrane potential and excitability of *Chara* cells with ATP and Mg^{2+} . J Membr Biol 37:167–192
Smith PT, Walker NA (1981) Studies on the perfused plasmalemma of *Chara corallina*:1. Current-voltage curves:ATP and potassium dependence. J Membr Biol 60:223–236
Sokolik AI, Yurin VM (1986) Potassium channels in plasmalemma of *Nitella* cells at rest. J Membr Biol 89:9–22
Staxen I, Pical C, Montgomery LT, Gray JE, Hetherington AM, McAinsh MR (1999) Abscisic acid induces oscillations in guard-cell cytosolic free calcium that involve phosphoinositide-specific phospholipase C. Proc Natl Acad Sci USA 96:1779–1784
Tazawa M, Kikuyama M (2003) Is Ca^{2+} release from internal stores involved in membrane excitation in characean cells? Plant Cell Physiol 44:518–526
Tazawa M, Kikuyama M, Shimmen T (1976) Electric characteristics and cytoplasmic streaming of *Characeae* cells lacking tonoplast. Cell Struct Funct 1:165–176
Tazawa M, Shimmen T, Mimura T (1987) Membrane control in the *Characeae*. Annu Rev Plant Physiol 38:95–117
Tazawa M, Yoko-o T, Mimura T, Kikuyama M (1994) Intracellular mobilization of Ca^{2+} and inhibition of cytoplasmic streaming induced by transcellular osmosis in internodal cells of *Nitella flexilis*. Plant Cell Physiol 35:63–72
Tester M (1990) Plant ion channels: whole-cell and single-channel studies. New Phytol 114:305–340
Thiel G, Dityatev AE (1998) Transient activity of excitatory Cl^- -channels in *Chara*: evidence for quantal release of a gating factor. J Membr Biol 163:183–191
Thomas MV (1982) Techniques in calcium research. Academic Press, London New York
Thuleau P, Schroeder JI, Ranjeva R (1998) Recent advances in the regulation of plant calcium channels: evidence for regulation by G-proteins, the cytoskeleton and second messengers. Curr Opin Plant Biol 1:424–427
Wacke M, Thiel G, Hütt M-T (2003) Ca^{2+} dynamics during membrane excitation of green alga *Chara*:model simulations and experimental data. J Membr Biol 191:179–192
Williamson RE (1975) Cytoplasmic streaming in *Chara*: a cell model activated by ATP and inhibited by cytochalasin B. J Cell Sci 17:655–665
Williamson RE, Ashley CC (1982) Free Ca^{2+} and cytoplasmic streaming in the alga *Chara*. Nature 296:647–651
Zherelova OM, Kataev AA, Berestovskii GN (1985) The necessity of ATP and Mg^{2+} for maintenance of the functional activity of the calcium channels of Charophyta algae. Doklady Biophys 280–282:37–39